Brain Structure and Function (2023) 228:1479–1492
https://doi.org/10.1007/s00429-023-02666-3

ORIGINAL ARTICLE

Using modular connectome-based predictive modeling to reveal brain-behavior relationships of individual differences in working memory

Huayi Yang[1,2] · Junjun Zhang[1] · Zhenlan Jin[1] · Pouya Bashivan[2,3] · Ling Li[1]

Received: 9 March 2023 / Accepted: 11 June 2023 / Published online: 22 June 2023
© The Author(s), under exclusive licence to Springer-Verlag GmbH Germany, part of Springer Nature 2023

Abstract
Working memory plays a crucial role in our daily lives, and brain imaging has been used to predict working memory performance. Here, we present an improved connectome-based predictive modeling approach for building a predictive model of individual working memory performance from whole-brain functional connectivity. The model was built using n-back task-based fMRI and resting-state fMRI data from the Human Connectome Project. Compared to prior models, our model was more interpretable, demonstrated a closer connection to the known anatomical and functional network. The model also demonstrates strong generalization on nine other cognitive behaviors from the HCP database and can well predict the working memory performance of healthy individuals in external datasets. By comparing the differences in prediction effects of different brain networks and anatomical feature analysis on n-back tasks, we found the essential role of some networks in differentiating between high and low working memory loads conditions.

Keywords Brain-behavior prediction · Connectome-based predictive modeling · Functional connectivity · Feature selection · Working memory

✉ Ling Li
liling@uestc.edu.cn

Huayi Yang
huayi.yang@std.uestc.edu.cn

Junjun Zhang
jjzhang@uestc.edu.cn

Zhenlan Jin
jinzl@uestc.edu.cn

Pouya Bashivan
pouya.bashivan@mcgill.ca

1 MOE Key Lab for NeuroInformation, High-Field Magnetic Resonance Brain Imaging Key Laboratory of Sichuan Province, Center for Psychiatry and Psychology, School of Life Science and Technology, University of Electronic Science and Technology of China, Chengdu 610054, China

2 Department of Physiology, McGill University, Montréal, QC H3G 1Y6, Canada

3 Mila, University of Montreal, Montréal, QC H2S 3H1, Canada

Introduction

Memory is a critical component in the study of cognitive function in the brain. Long-term episodic memory could be retained a long time and can be retrieved by the brain at any time. Working memory (WM), was first proposed, theorized and modeled in 1960, is a kind of short-term memory, which can temporarily maintain the information of the outside world and call other resources of the brain to process this information (Miller and Pribram 1960). Working memory is a system that specializes in maintaining and storing information in the short term and it is also a basic supporting structure of the thought process (Baddeley 2003). A temporary "workbench of cognition" in which information can operationally processed and assembled can be described as working memory (Klatzky 1975). The multicomponent model of working memory contains four components: the central executive, the phonological loop, the visuospatial sketchpad, and the episodic buffer (Baddeley 2000). It is commonly associated with intelligence, information processing, executive functioning, understanding, problem-solving, and learning, in infants to the elderly, and in a variety of animals (Cowan 2014).

The n-back task was developed to study short-term memory (Kirchner 1958). N-back task is a common experimental paradigm in the study of working memory (Redick and Lindsey 2013). In an n-back task, participants are presented with a series of visual or auditory stimuli (letters, numbers, or pictures) and during the task, decide whether the current stimulus matches the n previously presented stimuli. For example, in a 2-back task consisting of numbers, participants had to decide whether the current letter was the same as the one shown 2 time steps before. WM load can be controlled by the parameter n, the larger the n, the greater the memory load of the participants. The type of information stored in working memory and the complexity of the task have been found to affect the patterns of brain activation linked to N-back performance (Rottschy et al. 2012). Through studies using the n-back task, several brain regions have been identified that are associated with WM. For example, the lateral premotor cortex; dorsal cingulate and medial premotor cortex; dorsolateral and ventrolateral prefrontal cortex; frontal poles; and medial and lateral posterior parietal cortex are consistently activated during n-back to the task (Owen et al. 2005). Previous studies also have shown that different n showed different activated brain patterns in the n-back working memory paradigm, 2-back increased activation in left middle frontal gyrus, left inferior frontal gyrus and left anterior insula compared to 1-back (Wang et al. 2019).

Functional magnetic resonance imaging (fMRI) detects variations in blood flow to measure brain activity (Rinck 2014). The purpose of fMRI data analysis is to find correlations between brain activity and the tasks that subjects undertake during the scans. It also seeks to establish links between specific cognitive processes elicited in participants, such as memory and recognition (Logothetis 2008). Connectome-based predictive modeling (CPM) is a predictive modeling method for different cognitive functions and characteristics through whole-brain functional connectivity (Shen et al. 2017). It has been used to predict many cognitive functions, such as intelligence between males and females, full-scale and verbal intelligence in autism spectrum disorder, language processing and long-term memory (Dryburgh et al. 2020; Jiang et al. 2020a; Lin et al. 2020; Tomasi and Volkow 2020). Compared with traditional functional connectivity analysis, CPM provides an ideal framework to explore the "brain-behavior relationship", which fully considers all brain regions, and uses purely linear operations and data-driven methods to generate predictive models, thereby increasing the feasibility and interpretability of the models. In addition, cross-validation was used in CPM to help prevent potential errors inherent in whole-brain data-driven analysis and to increase the probability of replication in future studies (Shen et al. 2017; Sui et al. 2020). Many studies using functional links to predict behavior are based on resting-state fMRI data. However, studies have shown that task-based fMRI data can provide better prediction results (Jiang et al. 2020a).

In our research, we combined n-back task-based fMRI and resting-state fMRI data from the Human Connectome Project (HCP) to build models and used leave-one-out cross-validation to validate the model performance. By improving CPM, features from the brain's functional connections are more finely delineated, and the interpretation of model features is clearer on the basis of ensuring the model's predictive ability. Our model can accurately predict healthy individuals' working memory ability in both internal data sets and external validation sets. Our findings reveal brain regions and functional networks associated with working memory, as well as the role of brain networks in differentiating between high and low working memory loads. Furthermore, our research demonstrates the link between working memory and other cognitive abilities.

Materials and methods

Dataset 1: human connectome project S1200 release

The n-back task-based fMRI and resting-state fMRI data came from Human Connectome Project S1200 release (http://www.humanconnectome.org/), excluding subjects with either missing imaging data or missing behavioral data, a total of 874 subjects was used in the current study (470 females, 404 males, age 22–35). These subjects all performed the n-back task, and in the task, they are presented with blocks of trials that consisted of pictures of places, tools, faces and body parts and asked to monitor sequentially presented pictures (WU-Minn 2017). Within each session, half of the blocks are 2-back working-memory tasks and half are 0-back working-memory tasks. In HCP, MRI data were acquired on a 3T Siemens Skyra. By using a slice-accelerated, multiband, gradient-echo, echo planar imaging (EPI) sequence (TR = 720 ms, TE = 33.1 ms, flip angle = 52°, resolution = 2.0 mm^3, multiband factor = 8, left-right phase encoding, resting-state fMRI scan duration = 14:33, task-based fMRI scan duration = 5:01) the fMRI scans were collected. The T1-weighted structural scans were collected using a Magnetization Prepared Rapid Gradient Echo (MPRAGE) sequence (TR = 2400 ms, TE = 2.14 ms, TI = 1000 ms, resolution = 0.7 mm^3) (Van Essen et al. 2012).

The HCP data has been preprocessed using the HCP minimal preprocessing pipeline. The main preprocessing steps include (Glasser et al. 2013): gradient nonlinearity distortion; 6 degrees of freedom (DOF) FSL/FLIRT-based motion correction; FSL/top-up-based distortion correction; registration to a T1 space image; and FSL/FNIRT-based registration to MNI 2-mm space. We preprocessed HCP using methods that others had studied (Jiang et al. 2020b), to reduce low-frequency drift and high-frequency noise, we further band-pass-filtered the data at 0.009–0.08 Hz; the mean signal of the white matter, cerebrospinal fluid (CSF), and the movement parameters and its derivatives were regressed out as confounding factors; as well as removal of linear trend. After preprocessing, we separated the different tasks (0-back and 2-back) of task-based fMRI, then the whole brain was parcellated by using the Shen 268-node whole-brain atlas to define functional network nodes (Shen et al. 2013). EV (Explanatory Variable) files included in the dataset provide a set of conditions (and their associated timing) that can be used in the analysis of each task. According to the onset and duration of each task provided by the database, we can separate the signals of 0-back tasks and 2-back tasks. By calculating the Pearson correlation between each of 268 nodes of the whole brain, 268 × 268 symmetric functional connectivity matrices were created, then we used the Fisher transform to convert pearson *r*-values to *z*-values. For each subject, we used task-based fMRI and resting-state fMRI data, so two 268 × 268 symmetric functional connectivity matrices were created for each participant.

Dataset 2: conte center for the neuroscience of mental disorders

The external data set come from the Conte Center for the Neuroscience of Mental Disorders (CCNMD) at Washington University School of Medicine in St. Louis (Repovs et al. 2011). The task-based fMRI data set was obtained from the OpenfMRI database, its accession number is ds000115. Individuals diagnosed with schizophrenia, their unaffected siblings, and healthy controls performed three levels of an n-back task (0, 1 and 2-back). All participants took neuropsychological tests, 4 cognitive scores can be calculated, including intelligence quotient (IQ), working memory (WM), episodic memory and executive function, these cognitive scores are reported in Z scores relative to the mean of the entire sample (Delawalla et al. 2006; Repovš and Barch 2012). A total of 97 subjects were selected (39 females, 58 males, 74 healthy, 23 Schizophrenic, age 11–30). All scanning occurred on a 3T Tim TRIO Scanner at Washington University Medical School. Functional images (BOLD) were acquired using an asymmetric spin-echo, echo-planar sequence (T2*) (repetition time [TR] = 2500 ms, echo time [TE] = 27 ms, field of view [FOV] = 256 mm, flip=90°, voxel size = 4× 4× 4 mm). T1 structural image was acquired using a sagittal MP-RAGE 3D sequence (TR = 2400 ms, TE = 3.16 ms, flip = 8°; voxel size = 1 × 1 × 1 mm) (Repovs et al. 2011). Data preprocessing included: removal of first 5 images from each run, realignment, registration to a T1 space image, chose affine regularization in the segmentation with European, mean signal of the white matter, cerebrospinal fluid (CSF), and global were regressed out as confounding factors, removal of linear trend, normalize by using EPI template and band-pass-filtered the data at 0.009–0.08 Hz. Then the whole brain was parcellated by using the Shen 268-node whole-brain atlas to define functional network nodes (Shen et al. 2013).Mean regional time series were obtained by averaging voxel-wise fMRI time series in each of the 268 nodes for each individual. 268 × 268 symmetric functional connectivity matrices were created for each participant by calculating the Pearson correlation between each of 268 nodes of the whole brain and using the Fisher transform to convert pearson *r*-values to *z*-values.

Individualized prediction model

We applied the CPM with the d prime (d ’) of 0-back and 2-back tasks of working memory as behaviors and used the whole brain functional connectivity matrix from task-based fMRI and resting-state fMRI data to build the model and predict behaviors. 0-back and 2-back d-prime index using the hit rate (H) and false alarm rate (FA) to calculate, $d' = Z(H) - Z(FA)$, and Z means z-score transformation (Haatveit et al. 2010). Because d ’takes into account both "hit" and "false positives", it is more precise than accuracy values (Wu et al. 2021), and the higher the d’, the more accurate the response and the better the performance. Figure 1 demonstrates a summary of our prediction model. We made some improvements in feature selection to make the connection between the model and the brain network clearer and tighter. Firstly, when summarizing feature edges, the original method just divides them into the positive network and negative network for summation, and four feature values can be obtained for each subject: sumpos-task, sumneg-task, sumpos-rest, sumneg-rest (e.g., sumpos-task represents the sum of edges whose correlation *r* value is bigger than 0 and *p* value is less than the threshold, when task-based fMRI data are used to select significantly correlated edges). In our study, we divided the 268 nodes into 8 brain network regions according to the Shen 268 atlas (Finn et al. 2015), Fig. 2 is the Shen’s atlas categorizes 268 regions into eight networks. Compared with the original method of 4 features for each subject, the features of each subject are subdivided into 32. After feature summarization, correlation analysis between 32 characteristics of each subject and behavioral data was conducted again, then the top 8 most relevant features were found and newly selected features were used to build models. To identified the top 8 features, we ranked the features by their relevance to the behaviors.

Results

Individualized prediction

We used leave-one-out cross-validation to test the prediction effect of the CPM model and the improved model (threshold p <0.05, select edges that were positively and negatively correlated with behavior across individuals). The results are shown in Table 1, and the prediction effect is measured by the Pearson's correlations between observed and predicted scores and the root mean square error (RMSE). It can be seen that all models have a significant prediction effect on the d' of 0-back and 2-back working memory. Combining resting-state and task-based fMRI data or only using task-based fMRI data provided better predictive results than only resting-state fMRI data, this is consistent with the results

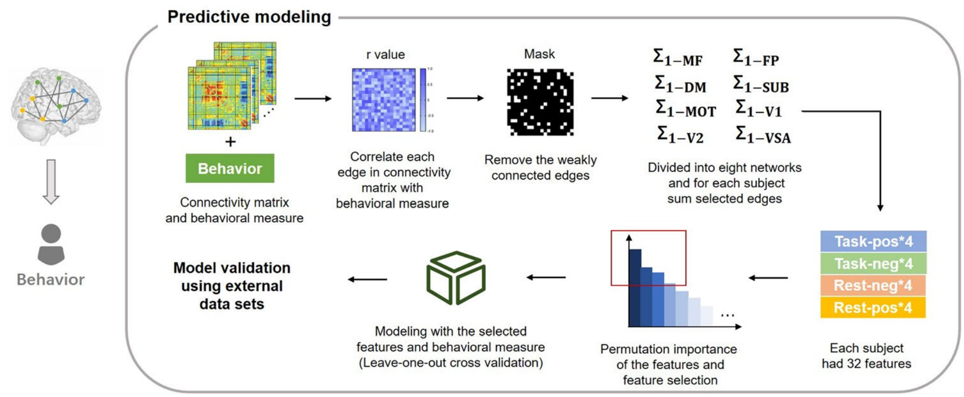

Fig. 1 Summary of the prediction model. We improved CPM, divided the feature values according to 8 brain network regions, and added the feature selection part. To connect brain functional connectivity with behavioral data, we combined n-back task-based fMRI and resting-state fMRI data for model building, and used external data sets to verify the model

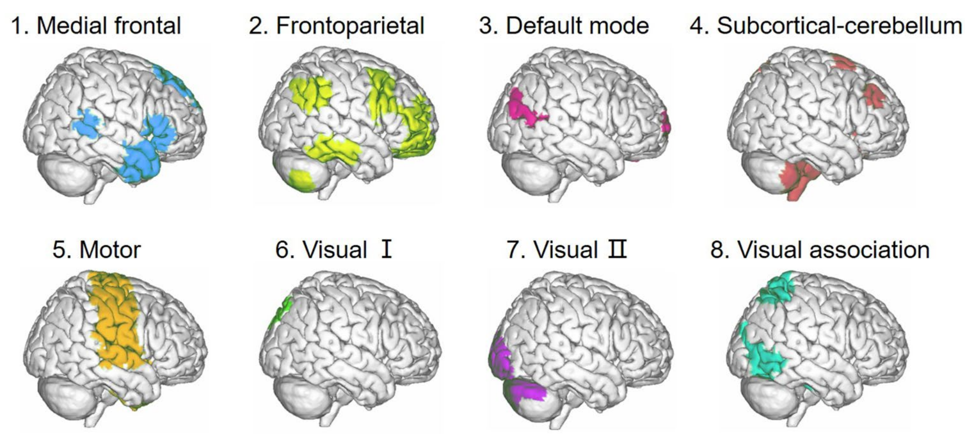

Fig. 2 Shen's atlas categorizes 268 regions into eight networks. The regions of the 8 networks were obtained from Shen 268 atlas. These networks include the medial frontal network, the frontoparietal network, the default mode network, the subcortical and cerebellar regions, the motor network, the visual I network, the visual II network, and the visual association network

Table 1 Prediction results of 0-back and 2-back d prime using CPM and 8-network-2FS

	Tasks	Model performance CPM	Model performance CPM-8-network-2FS
Resting-state fMRI data	0-back	$r = 0.1806$ $p = 7.6065 \times 10^{-08}$ RMSE = 1.6450	$r = 0.2185$ $p = 6.6347 \times 10^{-11}$ RMSE = 1.6372
Task-based fMRI data	0-back	$r = 0.5009$ $p = 1.0965 \times 10^{-56}$ RMSE = 1.4193	$r = 0.4991$ $p = 3.0662 \times 10^{-56}$ RMSE = 1.4206
Combining task-based and resting-state fMRI	0-back	$r = 0.4908$ $p = 3.6221 \times 10-54$ RMSE = 1.4307	$r = 0.5013$ $p = 8.2418 \times 10^{-57}$ RMSE = 1.4231
Resting-state fMRI data	2-back	$r = 0.1794$ $p = 9.3252 \times 10^{-08}$ RMSE = 1.3373	$r = 0.1635$ $p = 1.1779 \times 10^{-06}$ RMSE = 1.2199
Task-based fMRI data	2-back	$r = 0.4268$ $p = 5.3205 \times 10^{-40}$ RMSE = 1.2149	$r = 0.4214$ $p = 6.0608 \times 10^{-39}$ RMSE = 1.3614
Combining task-based and resting-state fMRI	2-back	$r = 0.4340$ $p = 1.9033 \times 10^{-41}$ RMSE = 1.2123	$r = 0.4224$ $p = 3.8257 \times 10^{-39}$ RMSE = 1.2208

of previous papers, which suggest that task-based brain connectivity can promote the detection of individual differences in brain–behavior relationships (Jiang et al. 2020b). However, there is little difference in the prediction results between using only resting-state fMRI data and combining resting-state and task-based fMRI data. Notably, combining task-based and resting-state fMRI and using the improved model for 0-back task can achieve great prediction results ($r[0-back] = 0.5013$, $p = 8.2418 \times 10^{-57}$, RMSE = 1.4231), combining task-based and resting-state fMRI and CPM can achieve great prediction results for 2-back task ($r[2-back] = 0.4340$, $p = 1.9033 \times 10^{-41}$, RMSE = 1.2123). From the results, we can know that improved model(CPM-8-Network-2FS) and original CPM model show little difference, and both of them can obtain significant prediction models with good performance. This suggests that our new model can enhance the association of the model with brain networks by separating features into different networks and analyzing them in detail without reducing the validity of the model. Therefore, to make the connection between the model and the brain network connections clearer, the improved model was used for all subsequent results.

To ensure that the constructed model has the strongest predictive ability, this study explores the influence of threshold values used in the threshold operation of the correlation matrix on the predictive ability of the model, that is, the predictive ability of the model constructed under different thresholds is quantitatively analyzed. We tested the performance of models at seven different thresholds (0.05, 0.01, 0.005, 0.001, 0.0005, 0.0001 and 0.00005; Fig. 3). The predictive power of the model peaked for the 0-back task at threshold = 0.0001 (0-back: $r = 0.5173$, $p = 5.6293 \times 10^{-61}$, RMSE = 1.4026). The predictive power of the model peaked for the 2-back task at threshold = 0.00005 (2-back: $r = 0.4536$, $p = 1.3989 \times 10^{-45}$, RMSE = 1.1958). We also tested the prediction ability of 0-back model on 2-back data and 2-back model on 0-back data respectively. The results show that both the 0-back model and the 2-back model can predict each other well (r[0-back model on 2-back data]= 0.3425, $p = 0.8369 \times 10^{-25}$, RMSE = 1.2852; Fig. 4c; r[2-back model on 0-back data] = 0.3178, $p = 5.8959 \times 10^{-22}$, $RMSE = 2.1859$; Fig. 4d). The following external dataset validation section used the optimal model obtained here by adjusting the threshold value. It can be noted that in the 0-bcak model, the observed scores are skewed high, but the predictions are symmetrically distributed. We think this is because the data we used are brain connectivity data, so that even if there are differences between each individual, they are not as different as behavioral data. In addition, the authors in the limitations section of the CPM paper also mention that prediction models tend to produce predicted values with ranges smaller than the range of true values (Shen et al. 2017). That is, the models overestimate the behavior of the individuals with the lowest measured values while underestimate. So, the predictive values derived through brain network connections are symmetric.

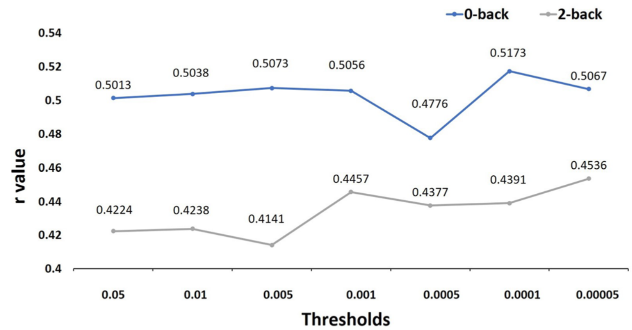

Fig. 3 Parameter optimization of the model. The predictive ability of the models constructed under seven different thresholds (p = 0.05, 0.01, 0.005, 0.001, 0.0005, 0.0001 and 0.00005) was analyzed. The predictive power of the model peaked for the 0-back task at threshold = 0.0001 (0-back: $r = 0.5173$, $p = 5.6293 \times 10^{-61}$, RMSE = 1.4026). The predictive power of the model peaked for the 2-back task at threshold = 0.00005 (2-back: $r = 0.4536$, $p = 1.3989 \times 10^{-45}$, RMSE = 1.1958)

Brain regions and functional networks that predict WM performance

Using the improved CPM, we elucidated the contribution of the eight different brain networks to working memory performance which enabled us to compare the differences between 0-back and 2-back tasks in utilizing these brain networks. Figure 5a shows the prediction results of leave-one-out cross-validation using 8 brain networks respectively, and the prediction effect is measured by r value. For 0-back task, subcortical and cerebellar regions, frontoparietal network, visual association network and motor network networks were the top predictive networks. For 2-back task, the most effective networks for model prediction were the frontoparietal network, default mode network, subcortical and cerebellar regions and visual association network, which would suggest that these brain networks are crucial for working memory. For statistical analysis, we divided the subjects randomly and equally into training and test sets, and this process was performed 500 times to obtain the model prediction performance r-values for 500, and we subsequently conducted a paired t-test on the prediction performance of the two tasks to explore whether there were significant differences in the prediction performance of different brain network regions in the two tasks. Table 2 shows the t-test results for significance and effect sizes Cohen's d. Through 500 times of two-fold cross-validation and T-test, we found significant differences in 0-back and 2-back working memory prediction ability for all eight networks. Although visual II network performed

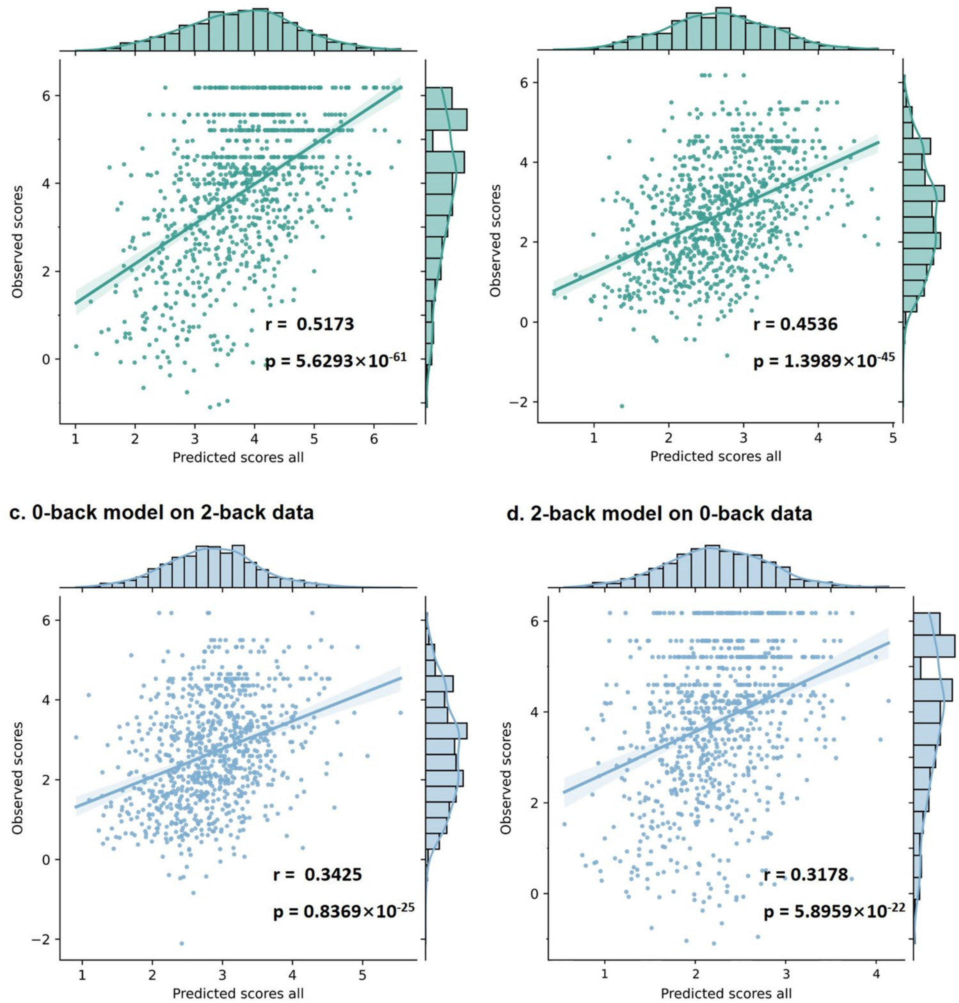

Fig. 4 Scatter plot of the model-estimated 0-back and 2-back d prime with respect to observed values. When integrating functional connectivity of task-based fMRI and resting-state fMRI features together as input for model, Pearson's correlations of r[0-back] = 0.5173 ($p = 5.6293 \times 10^{-61}$) and r[2-back] = 0.4536 ($p = 1.3989 \times 10^{-45}$) between predicted and observed scores were achieved for 0-back and 2-back task respectively. 0-back model and the 2-back model can predict each other well, r[0-back model on 2-back data] = 0.3425 ($p = 0.8369 \times 10^{-25}$) and r[2-back model on 0-back data] = 0.3178 ($p = 5.8959 \times 10^{-22}$)

better in 0-back tasks than 2-back in leave-one-out cross-validation, this was probably due to chance factors. In the results of 500 times of two-fold cross-validation and *T*-test, as shown in Fig. 5b, that visual II network performs better in the 2-back task. In general, the brain networks performed better on the 0-back task, the default mode network, visual I network and visual II network performed better on the 2-back network than the 0-back task (Fig. 5b).

To visualize the most predictive features and find the functional anatomy of positive and negative networks of WM task-trained and rest-trained WM model, we grouped the 268 nodes into 10 brain regions and 10 functional networks. Edge selection threshold for visualization is $p < 1 \times 10^{-4}$ for clarity. For 0-back tasks of WM task-trained, 1436 were selected in the positive network and 1194 edges were selected in the negative network. Nodes were mainly located in Prefrontal, L-Insula, R-MotorStrip, and L-Parietal (Fig. 6a). The positive networks were mainly concentrated in the motor network, and the negative networks were mainly concentrated in the motor, frontoparietal, visual association, salience limbic and medial frontal network (Fig. 7a). For 0-back tasks of rest-trained, 36 were selected in the positive network and 84 edges were selected in the negative network. Nodes were mainly in L-Prefrontal, L-Cerebellum, L-Limbic, L- Parietal and L-Prefrontal (Fig. 6a). The positive networks were mainly concentrated in the salience limbic, default mode and medial frontal network, and the negative networks were mainly concentrated in the motor, salience limbic, medial frontal and subcortical network (Fig. 7b). For 2-back tasks of WM task-trained, 1114 were selected in the positive network and 984 edges were selected in the negative network. Nodes were mainly located in Prefrontal and R-Temporal (Fig. 6b). The positive networks were mainly concentrated in the frontoparietal, salience limbic, default mode and medial frontal network, and the negative networks were mainly concentrated in the frontoparietal and salience limbic network (Fig. 7a). For 2-back tasks of rest-trained, 138 were selected in the positive network and 156 edges were selected in the negative network. Nodes were mainly distributed in R-Prefrontal, and some in L-Prefrontal, R-Parietal, L-Temporal, and R-Occipital (Fig. 6b). The positive networks were mainly concentrated in the salience limbic, medial frontal

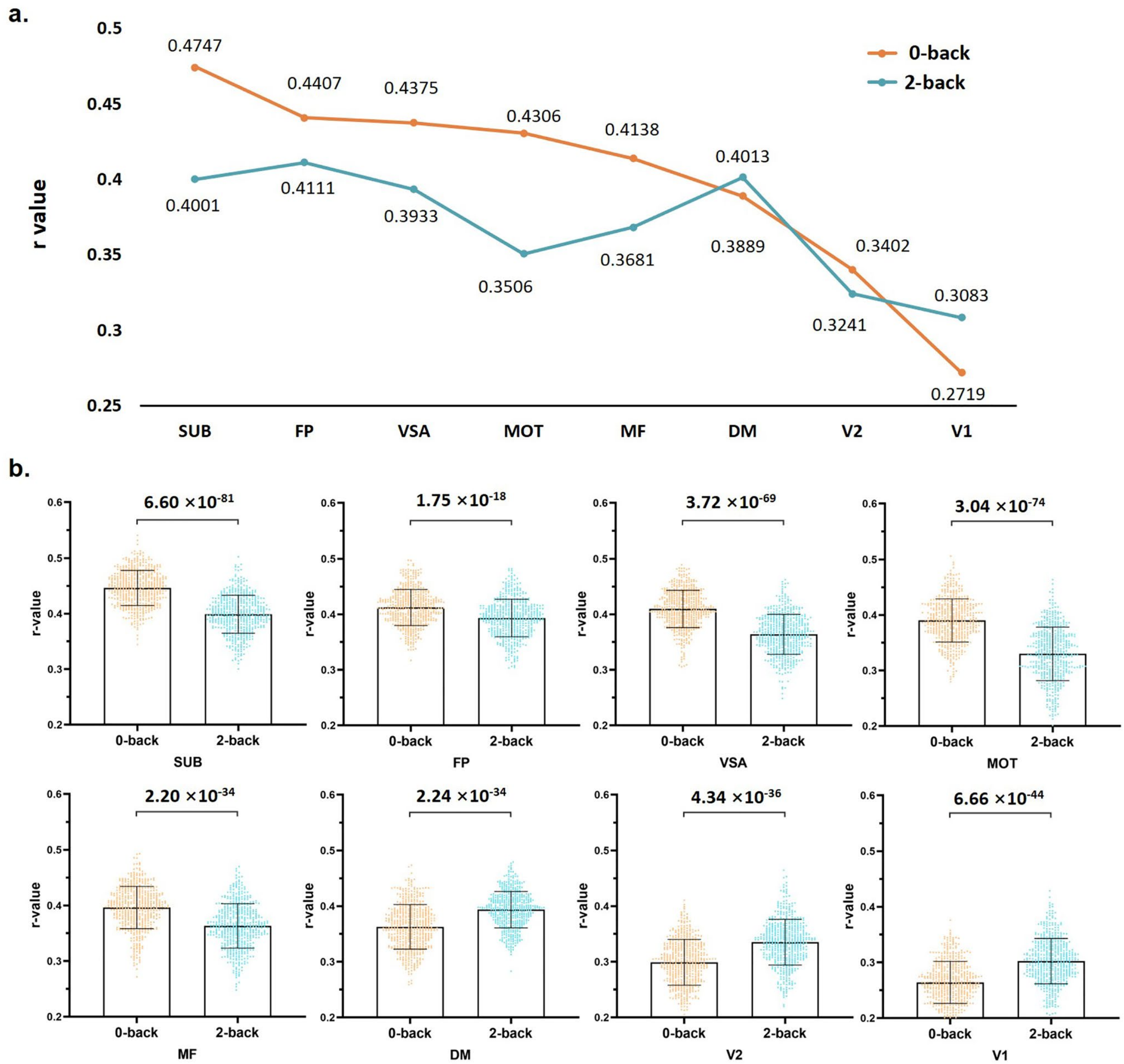

Fig. 5 Model performance of 8 brain network regions and the difference of 0-back and 2-back predicted contributions of different networks. The networks include the subcortical and cerebellar regions (SUB), the frontoparietal network (FP), the visual association network (VSA), the default mode network (DM), the medial frontal network (MF), the motor network (MOT), the visual II network (V2) and the visual I network (V1). **a** Prediction results of leave-one-out cross-validation using 8 brain networks respectively (threshold $p < 0.05$). Subcortical and cerebellar regions, frontoparietal network, visual association network and motor network were predicted better than other networks for the 0-back task. Subcortical and cerebellar regions, frontoparietal network, visual association network and the default mode network are the most effective networks for model prediction in the 2-back task. **b** The 500 times two-fold cross-validation and T-test results. Default mode network, visual I network and visual II network differed more noticeably across the two tasks

and default mode network, and the negative networks were mainly concentrated in the salience limbic, frontoparietal and medial frontal network (Fig. 7b). Tables 3 and 4 provide more thorough details regarding nodes and networks, including MNI Coordinates and degrees. 10 brain regions and 10 functional networks is drawn according to the mapping website provided in the CPM paper (https://bioimagesuite-web.github.io/webapp/connviewer.html). The classification of the 10 regions in the mapping website just subdivide the subcortical and cerebellar regions (SUB) into Salience Limbic (SAL), Subcortical (SC) and Cerebellum (CBL).

Table 2 Results of *t*-test for the difference in prediction effects between 0-back and 2-back task in different brain networks

Brain networks	*T*-test	
	Significance	Cohen's d
Subcortical and cerebellar regions	6.60×10^{-81}	1.0337
Frontoparietal network	1.75×10^{-18}	0.4081
Visual association network	3.72×10^{-69}	0.9256
Motor network	3.04×10^{-74}	0.9724
Medial frontal network	2.20×10^{-35}	0.6013
Default mode network	2.24×10^{-34}	0.5907
Visual II network	4.34×10^{-36}	0.6085
Visual I network	6.66×10^{-44}	0.6871

Network overlap

To test the effect of the working memory model on other cognitive behaviors, we selected nine other cognitive behaviors from the HCP database, including episodic memory, executive function, executive function/inhibition, fluid intelligence, language/reading decoding, language/vocabulary comprehension, processing speed, sustained attention, verbal episode memory. Edge overlap was retrained for each task and then compared with the working memory task finding the overlapping edges to compare other cognitive and working memory differences in brain connectivity. However, when testing the generalizability of the model, the model effects were derived from predictions using the pre-trained working memory model and were not retrained again for different tasks, and the edge selection was also based on the pre-trained working memory model. So, the result can be a real generalization test. Table 5 and 6 are the nine cognitive behaviors predicted results by using models built on 0-back and 2-back WM task and their edge overlap with working memory (threshold p <0.05). The Jaccard index measures the similarity of a finite set of samples, so in addition to the number of edge overlaps, we also provide the Jaccard index for the set of edges of the working memory task and other tasks. The higher the Jaccard index, the more similar the two samples are. We found that the model has a significant prediction effect on all nine cognitive behaviors (p <0.05), and the more overlapping edges they have with working memory, the better the model prediction effect (Fig. 8). The best predictions are for Fluid intelligence (r[0-back] = 0.4026,

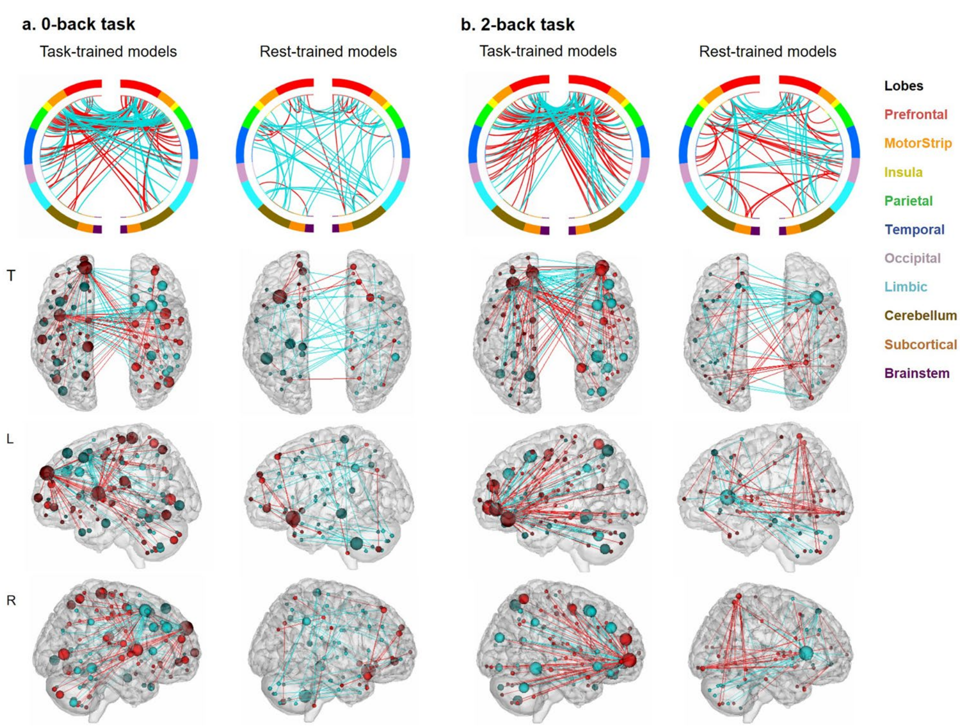

Fig. 6 Brain regions and functional connections predicting WM d prime in 10 brain lobes. We grouped the 268 nodes into 10 brain lobes: Prefrontal, MotorStrip, Insula, Parietal, Temporal, Occipital, Limbic, Cerebellum, Subcortical and Brainstem (threshold $p < 1 \times 10^{-4}$ when selected edges). The Circle plots show number of connections they have in both the positive and negative networks between the 10 brain lobes (red representing a positive network and blue representing a negative network). In the glass brain, lines indicate the edges, the size of the node represents the degree, indicating the total number of connections in the positive and negative networks, and is colored according to which network they have more connections in (red representing a positive network and blue representing a negative network)

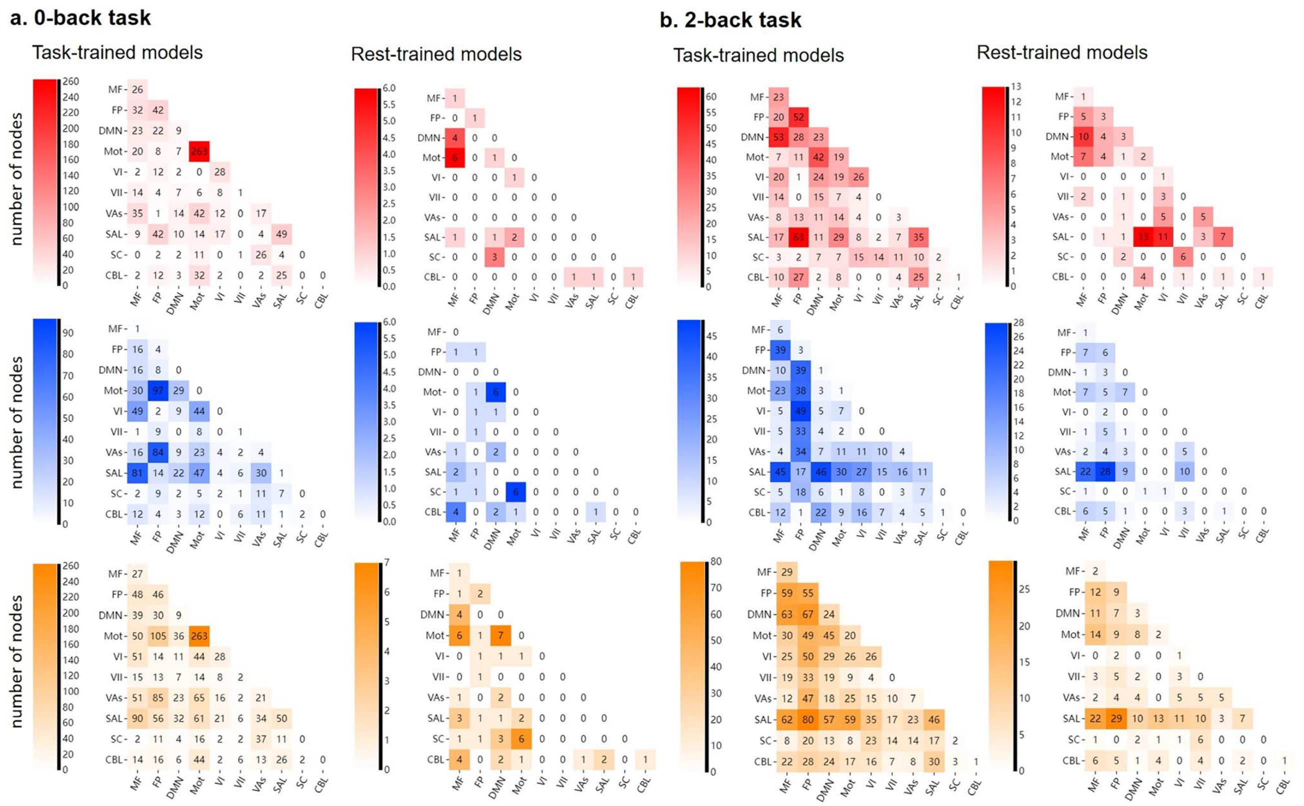

Fig. 7 Brain regions and functional connections predicting WM d prime in 10 networks of brain. In these matrix plots, rows and columns represent 10 networks of brain function, including Medial Frontal (MF), Frontoparietal (FP), Default Mode (DMN), Motor (Mot), Visual I (VI), Visual II (V II), Visual Association (VAs), Salience Limbic (SAL), Subcortical (SC) and Cerebellum (CBL). These cells represent the number of nodes in a positive and negative network (red representing a positive network, blue representing a negative network and orange representing the sum of positive and negative networks)

Table 3 The top five nodes with the strongest connections in the 0-back and 2-back task-trained prediction model

Task	Node	MNI coordinates (*x, y, z*)			Lobe	Degree	Network
0-back	Dorsolateral prefrontal cortex	−10.15	55.69	30.24	L-Prefrontal	53	Medial frontal
	Insular cortex	−39.09	1.71	9.54	L-Insula	48	Motor
	Premotor cortex and supplementary motor cortex	25.22	12.41	49.39	R-MotorStrip	45	Fronto- parietal
	Insular cortex	41.39	3.51	7.15	L-Insula	44	Motor
	Visuo-motor coordination	−7.35	−34.12	67.46	L-Parietal	43	Motor
2-back	Orbital part of inferior frontal gyrus	−28.35	36.03	−15.64	L-Prefrontal	55	Limbic
	Anterior prefrontal cortex	30.51	54.92	−3.52	R-Prefrontal	54	Fronto- parietal
	Anterior prefrontal cortex	−6.93	48.31	−5.71	L-Prefrontal	50	Default mode
	Fusiform gyrus	25.23	−44.56	−12.22	R-Temporal	48	Visual I
	Anterior prefrontal cortex	28.88	51.14	18.68	R-Prefrontal	47	Fronto- parietal

r[2-back] = 0.4080), language/vocabulary comprehension (r[0-back] = 0.3970, r[2-back] = 0.3743), Language/Reading Decoding and Executive Function (r[0-back] = 0.3662, r[2-back] = 0.3631), with a lot of overlapping edges, indicating a strong link between these behaviors with working memory.

External validation

To validate the model's performance on out of distribution samples, we use external data sets to further verify the model predictions. The external data were obtained from CCNMD, and a total of 97 subjects were selected

Table 4 The top five nodes with the strongest connections in the 0-back and 2-back rest-trained prediction model

Task	Node	MNI coordinates (x, y, z)			Lobe	Degree	Network
0-back	Orbital part of inferior frontal gyrus	−32.05	20.46	−15.97	L-Prefrontal	7	Medial frontal
	Cerebellum	−46.41	−46.77	−42.86	L-Cerebellum	6	Cerebellum
	Part of the perirhinal cortex	−20.71	−30.77	−11.12	L-Limbic	5	Basal ganglia
	Visuo-motor coordination	−7.35	−34.12	67.46	L-Parietal	4	Motor
	Anterior prefrontal cortex	−6.93	48.31	−5.71	L-Prefrontal	4	Default mode
2-back	Broca's area	36.98	20.81	5.89	R-Prefrontal	25	Limbic
	Frontal eye fields	−11.17	34.26	51.48	L-Prefrontal	11	Medial frontal
	Visuo-motor coordination	−25.17	−52.42	68.13	R-Parietal	10	Visual association
	Middle temporal gyrus	−59.85	−27.42	−18.14	L-Temporal	9	Fronto- parietal
	Secondary visual cortex(V2)	31.17	−91.77	−10.82	R-Occipital	9	Visual II

Table 5 Edge overlap of 0-back WM and other cognitions

Cognitions	Edge overlap with 0-back WM (Jaccard index) (task-pos; task-neg; rest-pos; rest-neg)				Model performance CPM-8-network-2FS
Fluid intelligence	4368 (0.3509)	3960 (0.3197)	1020 (0.1552)	1220 (0.1633)	$r = 0.4026$, $p = 4.8965 \times 10^{-35}$
Language/vocabulary comprehension	4080 (0.3281)	4000 (0.3266)	1050 (0.1492)	1110 (0.1454)	$r = 0.3970$, $p = 4.9063 \times 10^{-34}$
Language/reading decoding	3610 (0.2809)	3708 (0.2952)	872 (0.1349)	1056 (0.1476)	$r = 0.3662$, $p = 7.7715 \times 10^{-29}$
Executive function	2564 (0.2237)	2664 (0.2379)	736 (0.1142)	1044 (0.1462)	$r = 0.3165$, $p = 1.4166 \times 10^{-21}$
Processing speed	2324(0.2129)	2130 (0.2003)	776 (0.1035)	958 (0.1111)	$r = 0.2705$, $p = 5.6519 \times 10^{-16}$
Episodic memory	2602 (0.2334)	2024 (0.1791)	644 (0.1041)	766 (0.1102)	$r = 0.2613$, $p = 5.6538 \times 10^{-15}$
Executive function/inhibition	1946 (0.1785)	1586 (0.1479)	534 (0.0885)	680 (0.0998)	$r = 0.2059$, $p = 9.8605 \times 10^{-10}$
Verbal episode memory	980 (0.0939)	1022 (0.0981)	314 (0.0575)	512 (0.0824)	$r = 0.1606$, $p = 1.0888 \times 10^{-06}$
Sustained attention	840 (0.0798)	984 (0.0948)	368 (0.0614)	476 (0.0691)	$r = 0.1036$, $p = 2.2937 \times 10^{-03}$

Table 6 Edge overlap of 2-back WM and other cognitions

Cognitions	Edge overlap with 2-back WM (Jaccard index) (task-pos; task-neg; rest-pos; rest-neg)				Model performance CPM-8-network-2FS
Fluid intelligence	4138 (0.3593)	3778 (0.3467)	1420 (0.1999)	1472 (0.1890)	$r = 0.4080$, $p = 4.9299 \times 10^{-36}$
Language/vocabulary comprehension	3618 (0.2981)	3454 (0.2985)	1418 (0.1866)	1370 (0.1725)	$r = 0.3743$, $p = 3.6907 \times 10^{-30}$
Language/reading decoding	3444 (0.2969)	3422 (0.3092)	1294 (0.1856)	1356 (0.1827)	$r = 0.3632$, $p = 2.3099 \times 10^{-28}$
Executive function	2780 (0.2531)	2834 (0.2680)	1092 (0.1556)	1312 (0.1763)	$r = 0.3383$, $p = 1.3305 \times 10^{-24}$
Processing speed	2616 (0.2404)	2710 (0.2568)	996 (0.1473)	1014 (0.1394)	$r = 0.2912$, $p = 2.2617 \times 10^{-18}$
Episodic memory	2394 (0.2164)	2444 (0.2322)	1276 (0.1610)	1274 (0.1435)	$r = 0.2833$, $p = 2.0013 \times 10^{-17}$
Executive function/inhibition	2232 (0.2112)	1918 (0.1893)	726 (0.1072)	786 (0.1080)	$r = 0.2379$, $p = 1.3435 \times 10^{-12}$
Verbal episode memory	620 (0.0603)	512 (0.0518)	528 (0.0781)	688 (0.0950)	$r = 0.1395$, $p = 4.1081 \times 10^{-05}$
Sustained attention	740 (0.0752)	660 (0.0690)	432 (0.0689)	612 (0.0916)	$r = 0.1148$, $p = 7.1606 \times 10^{-04}$

(39 females, 58 males, 74 healthy, 23 Schizophrenic, age 11–30). Since the modeling data and the external validation data come from different databases, the two preprocessing processes are slightly different, see the Method section for details. Applying the 0-back and 2-back task-trained models to task-based functional connectivity from these individuals (0-back model: threshold = 0.0001; 2-back model: threshold = 0.00005), we found that the model established for the 0-back task could significantly predict the working memory and executive function of healthy individuals from CCNMD, and for the 2-back task model, healthy individuals' working memory, executive function and IQ can be significantly predicted (Table 7). Although the model could not predict the working memory of schizophrenics, there was a significant effect when schizophrenic and healthy individuals were combined,

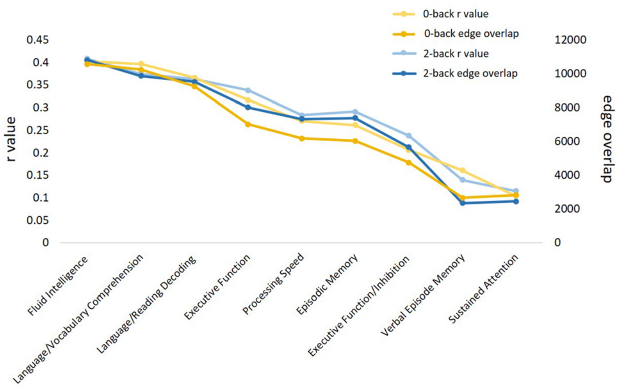

Fig. 8 Edge overlap and *r* value of 0-back and 2-back WM and other cognitions. The *R*-value calculation used the working memory model to predict other cognitive performance separately, and the edge overlap was the amount of overlap between the predicted edge of the working memory model and other cognitive behaviors when picked the edge of the prediction model (threshold = 0.05). The best predictions were for Fluid intelligence (r[0-back] = 0.4026, r[2-back] = 0.4080), language/vocabulary comprehension (r[0-back] = 0.3970, r[2-back] = 0.3743), Language/Reading Decoding and Executive Function (r[0-back] = 0.3662, r[2-back] = 0.3631)

which may be affected by the number of subjects. Therefore, we randomly selected 23 subjects from healthy individuals for prediction, randomly selected 100 times, and averaged the results. It can be seen that when the number of healthy subjects is reduced to 23, the model cannot significantly predict their behavior, suggesting that the number of subjects may have an impact on the predictive effect of the model. We also observed that the model had a significant predictive effect when the number of healthy subjects reached 55. And the model cannot generalize to schizophrenics also probably because the model was trained on data of the healthy. The result means that our model has a good predictive effect and good generalization ability on healthy individuals, 0-back WM model can predict working memory and executive function ability and the 2-back WM model can predict working memory, executive function and IQ.

Discussion

In this study, we used the task-based and resting-state functional connection matrices of 874 subjects from the Human Connectome Project dataset to establish working memory prediction models for 0-back and 2-back tasks. In the process of model building, we improved the CPM method, we subdivide the features according to the functional brain networks, rather than just adding them together as in the original CPM approach, and each brain region can be predicted separately and the predictions can be compared. This can give us a clearer understanding of the importance of different brain networks in working memory and make the model more closely related to brain connectivity. According to the results of the leave-one-out cross-validation, our model performed well at predicting individual working memory performance, was easier to interpret, and had a stronger relationship to the brain network. Furthermore, the model has greater potential for enhancement as the number of features increases from four to thirty-two. By using external data set validation from CCNMD, we demonstrated the validity of the model for predicting working memory ability on healthy individuals, as well as IQ, episodic memory and executive function. The model cannot be generalized to patients with schizophrenia, either because the model was trained on data from healthy individuals or because the amount of patient data is too small, which needs to be further explored in the future. Through exploring the prediction effect of working memory model on other cognitive behaviors, we found that the prediction ability of models is related to network overlap and the higher network overlap between a kind of cognitive behavior and working memory network, the stronger the prediction ability of working memory model for it. This finding demonstrates the close relationship between

Table 7 External validation of WM model

Task	Subjects	Working memory	Executive function	IQ	Episodic memory
0back	All	**$r = 0.2918$, $p = 0.0037$**	**$r = 0.3041$, $p = 0.0025$**	$r = 0.1347$, $p = 0.1883$	$r = 0.0796$, $p = 0.4383$
	Healthy	**$r = 0.3195$, $p = 0.0055$**	**$r = 0.3744$, $p = 0.0010$**	$r = 0.1508$, $p = 0.1998$	$r = 0.0633$, $p = 0.5922$
	Schizophrenic	$r = 0.3249$, $p = 0.1303$	$r = 0.2855$, $p = 0.1866$	$r = 0.0025$, $p = 0.9909$	$r = 0.2013$, $p = 0.3570$
	Healthy ($n = 23$)	$r = 0.2593$, $p = 0.3136$	$r = 0.3722$, $p = 0.1843$	$r = 0.1763$, $p = 0.4152$	$r = 0.1275$, $p = 0.5318$
	Healthy ($n = 55$)	$r = 0.2822$, $p = 0.1676$	**$r = 0.3841$, $p = 0.0363$**	$r = 0.2164$, $p = 0.1850$	$r = 0.1008$, $p = 0.5807$
2back	All	**$r = 0.3453$, $p = 0.0005$**	**$r = 0.4132$, $p = 0.00002$**	**$r = 0.2933$, $p = 0.0035$**	**$r = 0.2826$, $p = 0.0050$**
	Healthy	**$r = 0.2384$, $p = 0.0408$**	**$r = 0.3201$, $p = 0.0054$**	**$r = 0.2803$, $p = 0.0156$**	$r = 0.1663$, $p = 0.1566$
	Schizophrenic	$r = 0.3164$, $p = 0.1414$	$r = 0.3883$, $p = 0.0671$	$r = 0.0679$, $p = 0.7582$	$r = 0.1358$, $p = 0.5368$
	Healthy ($n = 23$)	$r = 0.2532$, $p = 0.3072$	$r = 0.2494$, $p = 0.2965$	$r = 0.3492$, $p = 0.1903$	$r = 0.2348$, $p = 0.3088$
	Healthy ($n = 55$)	**$r = 0.2386$, $p = 0.0411$**	**$r = 0.3229$, $p = 0.0463$**	$r = 0.2829$, $p = 0.1169$	$r = 0.2478$, $p = 0.1804$

Bold values indicate significant results ($p < 0.05$)

fluid intelligence, language/vocabulary comprehension, Language/Reading Decoding and Executive Function with working memory.

In the n-back working memory experiment, the 2-back task requires both attentional monitoring and working memory, while 0-back only requires attentional monitoring of the target, so the comparison of brain activation during 2-back versus 0-back can determine the regional response of working memory (Li et al. 2021). We used working memory d-prime to represent an individual's working memory performance. Anatomically, in both 0-back and 2-back tasks, a wide distribution of nodes was seen in the prefrontal cortex (PFC), which was consistent with the regional response to N-back memory described in previous studies: the prefrontal cortex is thought to be critical for the maintenance of elastic information during the working memory task (Funahashi et al. 1989; Fuster and Alexander 1971). In particular, there were a lot of nodes in Dorsolateral prefrontal cortex (DLPFC) in our results. DLPFC has often been reported in studies of working memory, and evidence from human functional neuroimaging and delayed response task studies in non-human primates suggests that DLPFC plays a crucial role in working memory (Bauer and Fuster 1976; Owen et al. 2005). The results of the 2-back task also revealed a wider distribution of nodes in the DLPFC than those from the 0-back task, highlighting the critical role the DLPFC plays in working memory. Although the rest-trained WM models showed higher number of connections between the ventrolateral prefrontal cortex (VLPFC) than DLPFC with other regions, this result is also reasonable, as VLPFC activation has been shown to occur in working memory activities in previous brain imaging studies (Wolf et al. 2006). As shown in our results, extensive connections between nodes in the parietal, temporal and cerebellum with other nodes were also observed in 2-back task, which are similar to brain regions reported in previous investigations of working memory. Like the PFC, the parietal cortex plays a significant role in working memory function and is essential for working memory information processing (Koenigs et al. 2009). Although the temporal lobe is not considered important in working memory, it has been shown to have sustained neural activity during working memory (Axmacher et al. 2007). And studies have shown that the cerebellum is linked to working memory (Zylberberg and Strowbridge 2017).

From the results of functional network, both in the 0-back task and 2-back task, we can see that the networks are more focused on the default mode and frontoparietal network, salience limbic and medial frontal. This is consistent with known research findings, studies have shown that dynamic signals between salience, frontoparietal, and default mode networks can predictive performance (Cai et al. 2021). In addition, connections within and between regions of the default mode network are highly utilized in predicting WM performance (Avery et al. 2020). The medial frontal is associated with the executive process (Talati and Hirsch 2005), so that part of the network connection may be due to the executive function being wanted in the working memory task. In particular, in the positive network of 0-back task-trained models, we notice that the number of nodes distributed in the motor network is much higher than the other networks and much higher than the number of nodes in the motor network of 0-back tasks. This conclusion is consistent with our findings in the network prediction section, where the motor network predicted the 0-back task significantly better than the 2-back task. Previous study has demonstrated that involvement of the motor system in working memory scales inversely with individual working memory capacity (Marvel et al. 2019). Similarly, based on our results, we believe that the use of the motor network is also inversely proportional to the working memory load.

The brain network region model performance outcomes are comparable to the network connectivity distribution results. Subcortical and cerebellar regions, frontoparietal network, visual association network and motor network predicted more accurately for the 0-back task than other networks. Subcortical and cerebellar regions, frontoparietal network, visual association network and the default mode network are the most successful networks for model prediction in the 2-back task, which suggests that these brain networks are essential for high load working memory task. Subcortical and cerebellar regions made the best contribution to the model in both n-back tasks, which are comparable to the findings reported in earlier studies: subcortical regions such as the cerebellum are indeed involved in working memory and some specific parts of the cerebellum are regulated by working memory load (Kirschen et al. 2005; Zylberberg and Strowbridge 2017). Interestingly, when comparing the difference in prediction results between the 0-back task and the 2-back task for each of the eight networks, although in general the brain networks performed better on the 0-back task, we discovered that the visual I network, visual II networks and default mode network performed better on the 2-back network than the 0-back task and the frontoparietal network is less different in the prediction of the two tasks. The 0-back task relies on detecting the stimulus that matches the target, while the 2-back task requires participants not only to detect and encode the incoming stimulus, but also to maintain and update the information. The 2-back task represents a higher working memory load compared to the 0-back task. This suggests that there may be functional differences between these brain networks in the 0-back and 2-back tasks. Studies have shown that the causal influence between multiple nodes in frontoparietal network, salience network and default mode network is modulated by high (2-back) and low (0-back) working-memory load conditions and predicts working memory performance, and communication between frontoparietal regions and the default mode network is essential for the appropriate load response (Cai et al. 2021; Eryilmaz et al. 2020). This provides support with the significant differences between default mode network and frontoparietal network in our predicted results for two tasks. Although visual I network and visual II networks did not perform as well as several other networks in predicting working memory, they showed significantly higher prediction performance in the high working memory load task than in the low working memory load task. Previous functional magnetic resonance imaging research revealed greater distractor competition effects on the sensory correlates in primary visual cortex (areas V1–V2) in conditions of high working memory load and high working memory load resulted in increased congruency-related functional connectivity between anterior cingulate cortex and V1 (Kelley and Lavie 2011). Our finding suggests that visual I network and visual II networks are associated with working-memory load conditions and they have a stronger network connectivity effect in high working memory loads. By comparing the prediction effects of these brain networks for 0-back and 2-back tasks, visual I network, visual II networks and default mode network showed better prediction effects in the 2-back task. In addition to demonstrating the important role of these networks in high working memory loads, since these networks can distinguish between high and low working-memory load conditions, they could be able to play an essential role in relevant predictive classification tasks in future studies.

Conclusion

In this study, we build models for predicting low and high working memory load (0-back and 2-back) working memory performance, the improved CPM makes the model more interpretable and more connected to the brain by subdividing the features into different brain networks. This allows us to compare the role of different networks in prediction and thus gain a clearer understanding of the role of different brain networks in working memory. And by increasing the number of model features, we provide more possibilities for future model improvement. We demonstrated the model's ability to generalize across different cognitive activities and to predict a wide range of healthy individuals by verifying its performance to be applied to other cognitive tasks and external data sets. In addition, a wide distribution of nodes was seen in the prefrontal, parietal, temporal and motor strip. And networks are mainly concentrated in the frontoparietal network, salience limbic, medial frontal and default mode network. These nodes and networks suggest a strong connection with working memory. By comparing the prediction effects of brain networks for 0-back and 2-back tasks, visual I network, visual II networks and default mode network demonstrated the important role in high working memory loads. Subcortical and cerebellar regions, frontoparietal network and visual association network predicted more accurately for both high and low working memory loads task than other networks, however, the motor network outperforms the default mode network for low working memory load and the default mode network for high working memory load. In summary, our model correlates resting-state and task-based fMRI with working memory behavior, and the model can well predict working memory performance and other behaviors closely associated with working memory. Unlike traditional fMRI research methods, we innovatively use CPM modeling approach to study high and low load working memory brain mechanisms. Our findings theoretically provide a wealth of information on the neural infrastructure of the WM process, including high and low working memory loads, that can help us better understand the neuroimage correlations behind working memory.

Author contributions HY wrote the main manuscript text. All authors reviewed the manuscript and made revisions to the manuscript.

Funding This research was supported by grants from NSFC (62176045), by Sichuan Science and Technology Program (2023YFS0191),111 project (B12027), and the Fundamental Research Funds for the Central Universities (ZYGX2020FRJH014).

Data availability The data that support the findings of this study are openly available in Human Connectome Project S1200 release at [http://www.humanconnectome.org/] and OpenfMRI database at [https://www.openfmri.org/] (accession number is ds000115).

Declarations

Conflict of interest The authors declare no competing interests.

References

Avery EW, Yoo K, Rosenberg MD, Greene AS, Gao S, Na DL, Scheinost D, Constable TR, Chun MM (2020) Distributed patterns of functional connectivity predict working memory performance in novel healthy and memory-impaired individuals. J Cogn Neurosci 32(2):241–255

Axmacher N, Mormann F, Fernández G, Cohen MX, Elger CE, Fell J (2007) Sustained neural activity patterns during working memory in the human medial temporal lobe. J Neurosci 27(29):7807–7816

Baddeley A (2000) The episodic buffer: a new component of working memory? Trends Cogn Sci 4(11):417–423

Baddeley A (2003) Working memory: looking back and looking forward. Nat Rev Neurosci 4(10):829–839

Bauer RH, Fuster JM (1976) Delayed-matching and delayed-response deficit from cooling dorsolateral prefrontal cortex in monkeys. J Comp Physiol Psychol 90(3):293

Cai W, Ryali S, Pasumarthy R, Talasila V, Menon V (2021) Dynamic causal brain circuits during working memory and their functional controllability. Nat Commun 12(1):1–16

Cowan N (2014) Working memory underpins cognitive development, learning, and education. Educ Psychol Rev 26(2):197–223
Delawalla Z, Barch DM, Fisher Eastep JL, Thomason ES, Hanewinkel MJ, Thompson PA, Csernansky JG (2006) Factors mediating cognitive deficits and psychopathology among siblings of individuals with schizophrenia. Schizophr Bull 32(3):525–537
Dryburgh E, McKenna S, Rekik I (2020) Predicting full-scale and verbal intelligence scores from functional connectomic data in individuals with autism spectrum disorder. Brain Imaging Behav 14(5):1769–1778
Eryilmaz H, Dowling KF, Hughes DE, Rodriguez-Thompson A, Tanner A, Huntington C, Coon WG, Roffman JL (2020) Working memory load-dependent changes in cortical network connectivity estimated by machine learning. Neuroimage 217:116895
Finn ES, Shen X, Scheinost D, Rosenberg MD, Huang J, Chun MM, Papademetris X, Constable RT (2015) Functional connectome fingerprinting: identifying individuals using patterns of brain connectivity. Nat Neurosci 18(11):1664–1671
Funahashi S, Bruce CJ, Goldman-Rakic PS (1989) Mnemonic coding of visual space in the monkey's dorsolateral prefrontal cortex. J Neurophysiol 61(2):331–349
Fuster JM, Alexander GE (1971) Neuron activity related to short-term memory. Science 173(3997):652–654
Glasser MF, Sotiropoulos SN, Wilson JA, Coalson TS, Fischl B, Andersson JL, Xu J, Jbabdi S, Webster M, Polimeni JR (2013) The minimal preprocessing pipelines for the human connectome project. Neuroimage 80:105–124
Haatveit BC, Sundet K, Hugdahl K, Ueland T, Melle I, Andreassen OA (2010) The validity of d prime as a working memory index: results from the "Bergen n-back task." J Clin Exp Neuropsychol 32(8):871–880
Jiang R, Calhoun VD, Cui Y, Qi S, Zhuo C, Li J, Jung R, Yang J, Du Y, Jiang T (2020a) Multimodal data revealed different neurobiological correlates of intelligence between males and females. Brain Imaging Behav 14(5):1979–1993
Jiang R, Zuo N, Ford JM, Qi S, Zhi D, Zhuo C, Xu Y, Fu Z, Bustillo J, Turner JA (2020b) Task-induced brain connectivity promotes the detection of individual differences in brain-behavior relationships. Neuroimage 207:116370
Kelley TA, Lavie N (2011) Working memory load modulates distractor competition in primary visual cortex. Cereb Cortex 21(3):659–665
Kirchner WK (1958) Age differences in short-term retention of rapidly changing information. J Exp Psychol 55(4):352
Kirschen MP, Chen SA, Schraedley-Desmond P, Desmond JE (2005) Load-and practice-dependent increases in cerebro-cerebellar activation in verbal working memory: an fmri study. Neuroimage 24(2):462–472
Klatzky RL (1975) Human memory: structures and processes. W. H. Freeman, P87
Koenigs M, Barbey AK, Postle BR, Grafman J (2009) Superior parietal cortex is critical for the manipulation of information in working memory. J Neurosci 29(47):14980–14986
Li G, Chen Y, Le TM, Wang W, Tang X, Li C-SR (2021) Neural correlates of individual variation in two-back working memory and the relationship with fluid intelligence. Sci Rep 11(1):1–13
Lin Q, Yoo K, Shen X, Constable RT, Chun MM (2020) A connectome-based prediction model of long-term memory. bioRxiv
Logothetis NK (2008) What we can do and what we cannot do with fmri. Nature 453(7197):869–878
Marvel CL, Morgan OP, Kronemer SI (2019) How the motor system integrates with working memory. Neurosci Biobehav Rev 102:184–194
Miller G-G, Pribram E (1960) vol 16. Henry Holt and company, New York
Owen AM, McMillan KM, Laird AR, Bullmore E (2005) N-back working memory paradigm: a meta-analysis of normative functional neuroimaging studies. Hum Brain Mapp 25(1):46–59
Redick TS, Lindsey DR (2013) Complex span and n-back measures of working memory: A meta-analysis. Psychon Bull Rev 20(6):1102–1113
Repovš G, Barch DM (2012) Working memory related brain network connectivity in individuals with schizophrenia and their siblings. Front Hum Neurosci 6:137
Repovs G, Csernansky JG, Barch DM (2011) Brain network connectivity in individuals with schizophrenia and their siblings. Biol Psychiat 69(10):967–973
Rinck P (2014) Magnetic resonance: a critical peer-reviewed introduction. Magnetic resonance in medicine. The basic textbook of the European magnetic resonance forum. BoD Germany, p 21
Rottschy C, Langner R, Dogan I, Reetz K, Laird AR, Schulz JB, Fox PT, Eickhoff SB (2012) Modelling neural correlates of working memory: a coordinate-based meta-analysis. Neuroimage 60(1):830–846
Shen X, Tokoglu F, Papademetris X, Constable RT (2013) Groupwise whole-brain parcellation from resting-state fmri data for network node identification. Neuroimage 82:403–415
Shen X, Finn ES, Scheinost D, Rosenberg MD, Chun MM, Papademetris X, Constable RT (2017) Using connectome-based predictive modeling to predict individual behavior from brain connectivity. Nature Protoc 12(3):506–518
Sui J, Jiang R, Bustillo J, Calhoun V (2020) Neuroimaging-based individualized prediction of cognition and behavior for mental disorders and health: methods and promises. Biol Psychiat 88(11):818–828
Talati A, Hirsch J (2005) Functional specialization within the medial frontal gyrus for perceptual go/no-go decisions based on what, when, and where related information: an fmri study. J Ccogn Neurosci 17(7):981–993
Tomasi D, Volkow ND (2020) Network connectivity predicts language processing in healthy adults. Hum Brain Mapp 41(13):3696–3708
Van Essen DC, Ugurbil K, Auerbach E, Barch D, Behrens TE, Bucholz R, Chang A, Chen L, Corbetta M, Curtiss SW (2012) The human connectome project: a data acquisition perspective. Neuroimage 62(4):2222–2231
Wang H, He W, Wu J, Zhang J, Jin Z, Li L (2019) A coordinate-based meta-analysis of the n-back working memory paradigm using activation likelihood estimation. Brain Cogn 132:1–12
Wolf RC, Vasic N, Walter H (2006) Differential activation of ventrolateral prefrontal cortex during working memory retrieval. Neuropsychologia 44(12):2558–2563
Wu Q, Ripp I, Emch M, Koch K (2021) Cortical and subcortical responsiveness to intensive adaptive working memory training: an mri surface-based analysis. Hum Brain Mapp 42(9):2907–2920
WU-Minn H (2017) 1200 subjects data release reference manual. URL https://www.humanconnectome.org. Accessed Nov 2021
Zylberberg J, Strowbridge BW (2017) Mechanisms of persistent activity in cortical circuits: possible neural substrates for working memory. Annu Rev Neurosci 40:603

Publisher's Note Springer Nature remains neutral with regard to jurisdictional claims in published maps and institutional affiliations.

Springer Nature or its licensor (e.g. a society or other partner) holds exclusive rights to this article under a publishing agreement with the author(s) or other rightsholder(s); author self-archiving of the accepted manuscript version of this article is solely governed by the terms of such publishing agreement and applicable law.